

Floquet Time Spirals and Discrete Time Quasi-Crystals

Hongzheng Zhao,¹ Florian Mintert,¹ and Johannes Knolle¹

¹*Blackett Laboratory, Imperial College London, London SW7 2AZ, United Kingdom*

(Dated: August 12, 2022)

We analyse quasi-periodically driven quantum systems that can be mapped exactly to periodically driven ones and find *Floquet Time Spirals* in analogy with spatially incommensurate spiral magnetic states. Generalising the mechanism to many-body systems we discover that a form of discrete time-translation symmetry breaking can also occur in quasi-periodically driven systems. We construct a discrete time quasi-crystal stabilised by many-body localisation, which persists also under perturbations that break the equivalence with periodic systems.

The dynamics of a quantum system governed by a generic time-dependent Hamiltonian is generally hard to analyse because to reach a certain point in time the entire history of evolution is required. Hence, simulations quickly become computationally unfeasible, especially for many-body systems. There are some exceptions such as periodically driven (PD) systems, i.e. whose Hamiltonian is periodic in time $H(t+T) = H(t)$, for which Floquet theory significantly reduces the effort to simulate the dynamics by decomposing the wave function to Floquet modes periodic over one time period T up to phases. PD systems are of immense recent interest as they have been exploited extensively for engineering sought after Hamiltonians [1–5], controlling quantum systems [6–14] and realising non-equilibrium quantum phases [15–17]. For instance, the proper combination of periodic driving and disorder in many-body localised systems [18] gave birth to the discovery of discrete time crystals (DTCs) [19–26], a new quantum phase with broken discrete time translation symmetry. An intriguing question is whether quasi-periodically driven (QPD) systems show features similar to time-crystalline behaviour of periodically driven systems? Generally such a question is hard to answer because Floquet theory, which provides an elegant framework for the analysis of periodically driven quantum systems normally does not generalise to aperiodic time-dependencies.

Here, we study a class of QPD systems which can be efficiently treated within Floquet theory. An originally QPD Hamiltonian H can be mapped exactly to a periodic counterpart \tilde{H} in a rotated frame as

$$\tilde{H}(t) = UH(t)U^\dagger - iU\partial_t U^\dagger, \quad (1)$$

via time-dependent unitary transformations $U(t)$. After solving the dynamics governed by the periodic Hamiltonian, the time-evolution in the original frame can be simply mapped back by applying the inverse of the unitary. The underlying idea – albeit with *site*-dependent instead of *time*-dependent unitaries – has been employed to study spiral magnetism in doped Hubbard models in the context of high-temperature cuprate superconductors [27–29] and with recent cold atom experiments [30]. For coplanar spirals the Hubbard model in the spin rotated

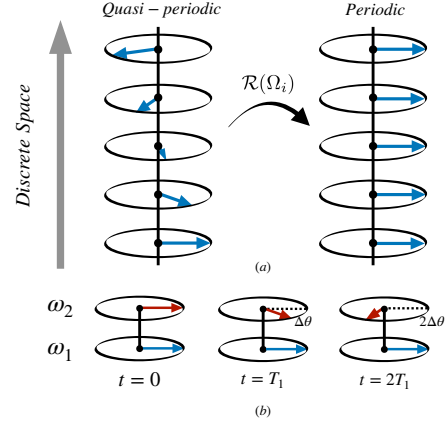


FIG. 1. (a) Mapping a quasi-periodic magnetic spiral to a periodic ferromagnet. (b) Illustration of the two components of the QPD Hamiltonian on the Bloch sphere. The vectors represent the driving fields in opposite directions with distinct frequencies $\omega_{1/2}$. The blue comes back to the original configuration at multiple periods nT_1 , while the red one with frequency ω_2 never comes back with mismatched angle $n\Delta\theta$.

frame becomes translationally invariant efficiently treatable via Bloch waves even for incommensurate spirals. Translating these ideas to the time domain of QPD systems allows us to construct *Floquet time spirals* (FTSs).

We provide an elementary example of a FTS via a two level system driven by two incommensurate frequencies which can be mapped to a periodic system. Generalising the idea to many-body systems we argue that a form of discrete time-translation symmetry breaking can also occur in QPD systems and we construct a minimal model of a discrete time quasi-crystal (DTQC). Crucially, we show that its appearance is not necessarily limited to the situations that are equivalent to a Floquet-problem, but we demonstrate that systems with many-body localisation show the DTQC behaviour even if perturbations break this equivalence. As such, the exact solvability of the models derived with our present construction allows us to gain clear physical insight into phenomena that extends far beyond these special cases.

We are interested in QPD systems which can be defined

via a Fourier expansion of the Hamiltonian [31–33]

$$H(t) = \sum_{\vec{n}} H_{\vec{n}} e^{i\vec{n} \cdot \vec{\theta}_t}, \quad (2)$$

with $\vec{n} = (n_1, n_2, n_3, \dots) \subseteq \mathbf{Z}^N$ and $\theta_{t,i} = \omega_i t$, where all or a subset of the N frequencies ω_i are incommensurate, i.e. their mutual ratios are irrational. There are some approaches to analyse QPD systems by mappings to higher dimensions [32, 34], constructing effective Hamiltonians to describe the system perturbatively [33], for analysing their asymptotic behaviour [35–38] or using them for enhanced performance of quantum simulations [39, 40] and creation of Majorana edge modes [41]. While in general for QPD systems we are lacking efficient methods for calculating their full time evolution, the FTSs introduced here are a special class corresponding to periodic systems in a rotating frame.

Our paper is organised as follows. First, we discuss the original idea of mapping quasi-periodic to periodic systems. Secondly, to elaborate our idea of FTSs we provide an elementary example of a QPD two-level system with analytic solutions. Finally, generalising our method to multiple interacting spins, we uncover the DTQC.

Mapping Quasi-Periodic to Periodic Systems. The basic idea goes back to studies of magnetic phases in Mott-Hubbard insulators, where incommensurate spiral magnetic states can be induced by doping [27–29]. For the description of spin-symmetry broken phases within the single band Hubbard model it is convenient to introduce site-dependent unitary transformations that locally rotates the spin quantisation axis, e.g. a unitary transformation $\mathcal{R}(\Omega_i) = e^{-i(\phi_i/2)\sigma_z} e^{-i(\theta_i/2)\sigma_y}$ with the spherical angles ϕ_i, θ_i for each operator $d_{i\eta}^\dagger = \sum_{\sigma} [\mathcal{R}(\Omega_i)]_{\eta\sigma} c_{i\sigma}^\dagger$ (with the standard creation operator $c_{i\sigma}^\dagger$ for a fermion at site \mathbf{r}_i with spin σ). The Hamiltonian (with nearest neighbour tunneling t , chemical potential μ and onsite interaction U) in the new frame reads

$$\begin{aligned} \tilde{H} = & -t \sum_{\langle ij \rangle, \sigma_1 \sigma_2} \left\{ d_{i,\sigma_1}^\dagger [\mathcal{R}^\dagger(\Omega_i) \mathcal{R}(\Omega_j)]_{\sigma_1 \sigma_2} d_{j,\sigma_2} + h.c. \right\} \\ & + U \sum_i d_{i,\uparrow}^\dagger d_{i,\uparrow} d_{i,\downarrow}^\dagger d_{i,\downarrow} + \mu \sum_{i,\sigma} d_{i\sigma}^\dagger d_{i\sigma}. \end{aligned} \quad (3)$$

Note the invariance of the Hubbard interaction and chemical potential term under the spin rotation. The important question in our context is whether we can still use Bloch's theorem and momentum as a good quantum number despite the site-dependent unitary transformation? It turns out that homogeneous co-planar spirals can still be efficiently described. Their oscillatory spiral spin order (with magnetization m) is of the form $\langle \mathbf{S}_i \rangle = m(\sin \theta_i, 0, \cos \theta_i)$, where $\theta_i = \mathbf{Q} \cdot \mathbf{r}_i$ defines the spiral wave number \mathbf{Q} . Note, for incommensurate spirals $(Q_x, Q_y)/(2\pi)$ is irrational and the unit cell is infinitely large. By setting $\phi_i = 0$ and $\theta_i = \mathbf{Q} \cdot \mathbf{r}_i$ in Eq.3 the unitary rotation aligns the spin axis with the spiral

and the kinetic term $\mathcal{R}^\dagger(\Omega_i) \mathcal{R}(\Omega_j) = e^{-i\mathbf{Q} \cdot (\mathbf{r}_i - \mathbf{r}_j) \sigma_y / 2}$ depends then only on the relative displacement $\mathbf{r}_i - \mathbf{r}_j$ and not on $\mathbf{r}_i, \mathbf{r}_j$ separately. Hence, the co-planar spiral maps to a ferromagnet (FM) in the new spin reference frame, see Fig.1(a). Crucially, the rotated Hamiltonian \tilde{H} becomes translationally invariant and with momentum as a good quantum number it can be conveniently described, e.g. in a mean-field treatment of the interaction [28].

The basic idea of mapping quasi-periodic to periodic systems can be extended to the time domain: We can construct instances of Hamiltonians $H(t)$, which are *aperiodic* in time such that $H(t) \neq H(t+T)$ for any T , but the time evolution of states $|\tilde{\phi}(t)\rangle = U(t)|\phi(t)\rangle$, which are rotated to a new frame via a time-dependent unitary transformation $U(t)$, is governed by a time *periodic* Hamiltonian with $\tilde{H}(t) = \tilde{H}(t+T)$. Here $|\phi(t)\rangle$ is the time dependent solution of the Schrödinger equation of the original system and it is easy to see [13] that the Hamiltonian in the rotated frame is given by Eq. 1.

In practise the construction is done in reverse such that any periodically time-dependent Hamiltonian helps to define an aperiodic Hamiltonian in terms of a time-dependent unitary transformation which allows us to analyse specific instances of quasi-periodic systems in terms of Floquet theory, and to understand their dynamics. Crucially, we show that some of the lessons learned from these specific instances directly translate to the general case where a mapping between periodic and quasi-periodic systems is missing. As such, we can use Floquet theory in order to understand the physics of systems to which Floquet theory fundamentally does not apply.

Floquet Time Spirals of a QPD Spin. As an elementary example of a FTS we study a QPD two-level system with two frequencies ω_1, ω_2 .

Consider the time-dependent Hamiltonian, $H(t) = H_1(t) + H_2(t)$, where H_1, H_2 describes two circular drivings

$$\begin{aligned} H_1(t) &= -\frac{A}{2} \cos(\omega_1 t) \sigma_z + \frac{A}{2} \sin(\omega_1 t) \sigma_y, \\ H_2(t) &= -\frac{A}{2} \cos(\omega_2 t) \sigma_z - \frac{A}{2} \sin(\omega_2 t) \sigma_y + \frac{\Omega}{2} \sigma_x, \end{aligned} \quad (4)$$

with Pauli matrices σ_α for $\alpha = x, y, z$ and the last term of strength $\Omega/2$ is a constant field in x direction. One can plot the two components of the time-dependent Hamiltonian on the Bloch sphere as conversely rotating vectors illustrated intuitively in Fig.1(b). We choose the driving component with ω_1 to set a discrete time coordinate (blue) which now plays the role of a lattice. Suppose the two frequencies are mutually incommensurate, the other rotating red vector with frequency ω_2 in Fig. 1 is aperiodic with a mismatched phase angle $n\Delta\theta = n\frac{\omega_2}{\omega_1}2\pi$ at discrete times nT_1 . According to the definition given in Eq. 2, the Hamiltonian is certainly quasi-periodic. Now the unitary transformation

$$U(t) = e^{i(\omega_1 - \omega_2)t\sigma_x/4}, \quad (5)$$

implements a rotation around the x -axis linearly changing in time and gives according to Eq. 1, the rotated Hamiltonian

$$\tilde{H}(t) = -A \cos(\omega t) \sigma_z + \left(\frac{\Omega}{2} - \frac{\omega_1 - \omega_2}{4}\right) \sigma_x. \quad (6)$$

It is simply a two-level system driven by a periodic field with frequency $\omega = (\omega_1 + \omega_2)/2$, which has been studied with Floquet theory extensively [42, 43]. For the sake of simplicity we have set $\Omega = (\omega_1 - \omega_2)/2$ such that the constant field vanishes and Floquet quasi-energies are zero, which permits an exact solution of the time evolution with

$$|\tilde{\phi}(t)\rangle = \sum_{\sigma} c_{\sigma}(t=0) \exp \left[i \text{sgn}[\sigma] \frac{A}{\omega} \sin(\omega t) \right] |\sigma\rangle, \quad (7)$$

where $\sigma = \uparrow, \downarrow$ and $\text{sgn}[\sigma]$ gives $+, -$ respectively. For an initial state with $c_{\sigma}(t=0) = 1/\sqrt{2}$ one readily obtains the magnetisation in the z direction

$$\begin{aligned} S^z(t) &= \langle \phi(t) | \sigma^z | \phi(t) \rangle = \langle \tilde{\phi}(t) | U(t) \sigma^z U^\dagger(t) | \tilde{\phi}(t) \rangle \\ &= -\sin(\Omega t) \sin \left[\frac{2A}{\omega} \sin(\omega t) \right], \end{aligned} \quad (8)$$

where the time dependence contains two independent frequencies, see inset of Fig. 2. Other observables, like non-equal time correlation function $S^{zz}(t, 0) = \langle \phi | \sigma^z(t) \sigma^z(0) | \phi \rangle = \cos(\Omega t) + i \sin(\Omega t) \cos \left[\frac{2A}{\omega} \sin(\omega t) \right]$ can be computed in a similar manner. Note, the imaginary part of this correlation function can be treated as a suitable measure for the quasi-periodicity. The dominating peaks in the frequencies spectrum of the magnetisation S^z , blue line of Fig. 2, are located at $\frac{k \pm 1}{2} \omega_1 + \frac{k \mp 1}{2} \omega_2$ or equivalently $k\omega \pm \Omega$ for odd integer k , ensuring that only integer multiples of $\omega_{1/2}$ appear like the first two blue peaks located at ω_1, ω_2 . This shows that the observable simply synchronises with the external drive as expected. The fact that the peaks of the Fourier decomposition of the Hamiltonian coincide with the one of the observables is a signature that the system preserves the long-range quasi-periodic time order imposed by the external drive, which is analogous to observables of well known spatial quasi-crystals which do not possess translational symmetry but are still long-range ordered [44]. However, an intriguing possibility would be the breaking of this QPD long-range order, i.e. Fourier peaks at half integer multiples of the driving frequencies may appear as discussed in the following section.

Discrete Time Quasi-Crystals. The idea of FTS can be generalised to study QPD many-body systems like interacting spin chains. Here, we focus on a new type of DTQC and discuss its rigidity which shows that it is robust beyond our method of construction.

First, let us formally define what we mean by the breaking of long-range quasi-periodic time order. Recall

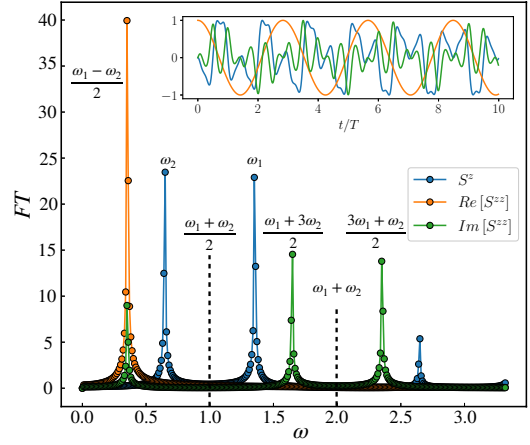


FIG. 2. QPD two-level system: Fourier transformation of the dynamics of observables computed by exact diagonalization for parameters $A = 1, \omega = 1, \Omega = \sqrt{2}/4$. Peaks of S^z appearing at $k\omega \pm \Omega$ for odd integer k suggests that the system synchronises with the external drive. Dashed lines labels the frequencies of observables in the rotating frame. The inset presents real time behaviour.

the usual definition of discrete time translational symmetry breaking (TTSB) [21]. For a PD system with period T , there exists an operator \hat{O} signalling TTSB if $\langle \hat{O} \rangle_t$ is only invariant under time translation by nT for $n > 1$ [45]. In contrast to PD systems, QPD systems do not have a well defined period but, loosely speaking [46], one can still define quasi-periodic time translation symmetry breaking (QTTSB) in terms of frequency. For instance, consider a QPD Hamiltonian defined by Eq. 2, TTSB occurs if for each t , there exists an operator $\langle \hat{O} \rangle_t$ with Fourier decomposition as

$$\langle \hat{O} \rangle_t = \sum_{\vec{n}} O_{\vec{n}} e^{i \sum_i n_i \omega_i / p_i t}, \quad (9)$$

with at least one of the non-negative integers p_i larger than 1. Basic TTSB in PD system is included in the above definition, i.e. period doubling with only one ω_0 and $p_0 = 2$. Note, our definition is different from a very recent proposal of time quasi-crystals in bosonic systems [47] where the frequency of the drive and of the observable are not simply related.

Combining a standard DTC model [20] with our FTS allows us to write down a QPD model realising QTTSB. The Hamiltonian is given by

$$H(t) = H_{MBL}(t) + H_d(t) + \frac{\Omega}{2} \sum_j \sigma_j^x, \quad (10)$$

where

$$H_{MBL}(t) = h_1(t) \sum_{j=1}^N [J_j \sigma_j^x \sigma_{j+1}^x - h_j^x \sigma_j^x], \quad (11)$$

with J_j, h_j^x chosen from uniform distributions. Disorder in nearest neighbour interactions and longitudinal fields

induces many-body localisation for generic small perturbations which prevents the system from heating to infinite temperature [16]. Each spin is subjected to a QPD field captured by

$$H_d(t) = h_2(t) \sum_j [\cos(\Omega t) \sigma_j^z - \sin(\Omega t) \sigma_j^y]. \quad (12)$$

The driving terms in the Hamiltonian are switched on and off periodically such that the stepwise function within one period $t \in (-T/2, T/2)$ read

$$h_1(t) = \begin{cases} 1, & |t| \leq \frac{T}{4} \\ 0, & |t| > \frac{T}{4} \end{cases}, \quad h_2(t) = \begin{cases} 0, & |t| \leq \frac{T}{4} \\ g, & |t| > \frac{T}{4} \end{cases}, \quad (13)$$

ensuring that the global rotation (determined by g) and the many-body localisation act on the system within different time windows. According to the definition Eq. 2, one can check the combined driving in Eq. 12, $h_2(t) \cos(\Omega t)$ or $h_2(t) \sin(\Omega t)$, is QPD by using the Fourier expansion of the box function, e.g.

$$h_2(t) \cos(\Omega t) = \sum_{n_1=-\infty}^{+\infty} \sum_{n_2=\pm 1} c_{n_1} e^{i(n_1 \omega + n_2 \Omega)t}, \quad (14)$$

with $\omega = 2\pi/T$ and coefficients $c_{n_1=0} = g/2$, and $-gsinc(n_1/2)/2$ for non-zero n_1 . According to Eq.1 the unitary transformation $U(t) = e^{i\frac{\Omega}{2}t \sum_j \sigma_j^x}$ gives the new Hamiltonian $\tilde{H}(t) = \tilde{H}_{MBL}(t) + \tilde{H}_d(t)$ written as

$$\tilde{H}(t) = h_1(t) \sum_j [J_z \sigma_j^x \sigma_{j+1}^x - h_j^x \sigma_j^x] + h_2(t) \sum_j \sigma_j^z. \quad (15)$$

In the rotated frame it is the standard model of a DTC with well-defined period T which for $g \approx \omega/2$ shows robust TTSB [20, 21]. It is clear that TTSB in the rotating frame translates into QTTSB in the original physical frame.

Signature of QTTSB and Rigidity. QTTSB can be observed from the expectation values of the spin operators $S^{y,z}(t)$ (σ^x commutes with the unitary transformation). In the following, we use ED to do numerical simulation given parameters $J_i \in [1/2, 3/2]$, $h_j^x \in [0, 1]$, $\omega = 1$, $\Omega = \sqrt{2}/4$ with periodic boundary condition and trotter step $\Delta t = T/300$. The Fourier transformation of $S_y(t)$ is presented in Fig. 3. The subharmonic response w.r.t. the Fourier decomposition of the drive in Eq.14 is a clear signature of QTTSB with sharp peaks located at $k\omega/2 \pm \Omega$ for odd integer k .

Finally, we check the stability of the DTQC by probing the rigidity of the $k\omega/2 \pm \Omega$ subharmonic response in the Fourier spectrum. Of course, our system is stable against perturbations, namely the pulse imperfections in H_d or unwanted field disorders in H_{MBL} , which can be mapped to those studied before for the periodic system in the rotating frame [20, 21]. Our major concern – also

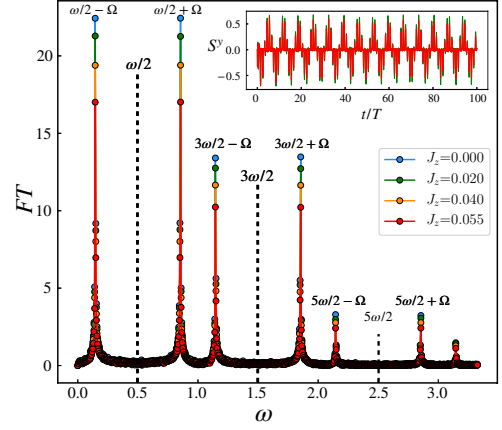


FIG. 3. Fourier transformation (FT) of the average magnetization in y direction of the DTQC, computed by ED with 10 sites (average over 300 disorder configurations) for different interaction perturbations J_z . FT is done with 200-400 T . For the system without perturbation, in the rotating frame, subharmonic behaviour can be identified by peaks at $k\omega/2$ with odd integer k labelled by the dashed line, whereas in the original frame, new peaks at $k\omega/2 \pm \Omega$, show the existence of the robust time quasi-crystal. Inset shows real time dynamics for $J_z = 0.02, 0.055$.

to show that the DTQC is more fundamental than our construction of mapping it to a DTC – are perturbations which can not be transformed to a simply periodic system in the rotating frame. For concreteness we focus on adding interaction perturbations $h_1(t) \sum_j J_z \sigma_j^z \sigma_{j+1}^z$ to H_{MBL} in Eq. 11 of uniform strength J_z , which do not commute with the unitary transformation. We plot the Fourier spectrum shown in Fig. 3 for various J_z , and the inset shows the quasi-periodically oscillating evolution of $S^y(t)$. Robust peaks are locked at $k\omega/2 \pm \Omega$ with descending heights for increasing perturbations. We find that for $J_z = 0.02$, the oscillations persist without decay up to at least $1000T$ (see also Supplementary Material (SM)), demonstrating that the DTQC is robust w.r.t. small perturbative interaction. The slight decay of the oscillating amplitude with $J_z = 0.055$ suggests that a thermalisation phase transition occurs and the system heats up. More detailed simulations and a discussion of finite size effects are given in the SM.

Discussion and Conclusion. Following an analogy with co-planar spiral magnets we have shown that certain QPD quantum systems can be mapped via suitably chosen time-dependent unitary transformations to PD ones. We discussed a form of time translation symmetry breaking in QPD systems, and discovered a new type of robust DTQC. We have also checked that the subharmonic response survives the presence of power-law decaying long-range interactions which suggests the feasibility of our proposal with current experimental setups of ion-trap quantum simulators [23–25].

From our examples it is clear that the QPD Hamiltonian and the unitary mapping are easiest obtained via backwards-engineering. We start from a periodic system of choice, apply a time-dependent unitary and arrive at the quasi-periodic system. The inverse transformation ensures that it can be mapped back. Because of this arguable fine-tuning, it was important to show that our DTQC is robust w.r.t. perturbations that do not permit a mapping to a periodic system, therefore, it is more fundamental than our construction. Thus, we have found a many-body quantum system driven by two incommensurate frequencies which avoids thermalisation.

We have restricted our basic examples to unitaries of spin rotations varying linearly in time but it would be interesting to construct QPD systems with more general time- and space-dependent transformations. A more ambitious goal would be to start from generic QPD systems and investigate the existence of maps to periodic ones. The concept of DTQC substantially enriches our understanding of discrete time translation symmetry and its breaking, indicating that subharmonic frequency response is more fundamental than period n -tupling [48] ill-defined for QPD systems in real time. Although the QTTSB can be expected with subharmonic responses associated with all primary frequencies, e.g. ω and Ω in our case, we only observe the QTTSB with $\omega/2$ but not Ω . It will be interesting to explore more general QTTSB and other DTQCs in the future.

Finally, it will be worthwhile to explore the underlying idea of mapping quasi-periodic systems to periodic ones in other contexts beyond the original spiral magnets or the time domain as presented here.

Acknowledgements. J.K. thanks Achilleas Lazarides and Shtitadi Roy for helpful discussions. H.Z. thanks Guanchen Peng for discussions. This work is part of the project TheBlinQC that has received funding from the QuantERA ERA-NET Cofund in Quantum Technologies implemented within the European Union's Horizon 2020 Programme.

[1] T. Oka and H. Aoki, Phys. Rev. B **79**, 081406 (2009).
[2] T. Kitagawa, E. Berg, M. Rudner, and E. Demler, Phys. Rev. B **82**, 235114 (2010).
[3] N. H. Lindner, G. Refael, and V. Galitski, Nature Physics **7**, 490 (2011).
[4] N. Goldman and J. Dalibard, Phys. Rev. X **4**, 031027 (2014).
[5] N. R. Cooper, J. Dalibard, and I. B. Spielman, Rev. Mod. Phys. **91**, 015005 (2019).
[6] H. Lignier, C. Sias, D. Ciampini, Y. Singh, A. Zenesini, O. Morsch, and E. Arimondo, Phys. Rev. Lett. **99**, 220403 (2007).
[7] M. Bukov, L. D'Alessio, and A. Polkovnikov, Advances in Physics **64**, 139 (2015).
[8] M. Holthaus, Journal of Physics B: Atomic, Molecular

and Optical Physics **49**, 013001 (2016).
[9] A. Verdeny and F. Mintert, Phys. Rev. A **92**, 063615 (2015).
[10] A. Verdeny and F. Mintert, Phys. Rev. A **92**, 033407 (2015).
[11] A. Eckardt, Rev. Mod. Phys. **89**, 011004 (2017).
[12] F. Meinert, M. J. Mark, K. Lauber, A. J. Daley, and H.-C. Nägerl, Phys. Rev. Lett. **116**, 205301 (2016).
[13] A. Eckardt, M. Holthaus, H. Lignier, A. Zenesini, D. Ciampini, O. Morsch, and E. Arimondo, Phys. Rev. A **79**, 013611 (2009).
[14] T. Oka and S. Kitamura, Annual Review of Condensed Matter Physics **10**, 387 (2019), <https://doi.org/10.1146/annurev-conmatphys-031218-013423>.
[15] M. Heyl, Reports on Progress in Physics **81**, 054001 (2018).
[16] V. Khemani, A. Lazarides, R. Moessner, and S. L. Sondhi, Phys. Rev. Lett. **116**, 250401 (2016).
[17] A. Lazarides, A. Das, and R. Moessner, Phys. Rev. E **90**, 012110 (2014).
[18] R. Nandkishore and D. A. Huse, Annu. Rev. Condens. Matter Phys. **6**, 15 (2015).
[19] B. Huang, Y.-H. Wu, and W. V. Liu, Phys. Rev. Lett. **120**, 110603 (2018).
[20] N. Y. Yao, A. C. Potter, I.-D. Potirniche, and A. Vishwanath, Phys. Rev. Lett. **118**, 030401 (2017).
[21] D. V. Else, B. Bauer, and C. Nayak, Phys. Rev. Lett. **117**, 090402 (2016).
[22] K. Giergiel, A. Miroszewski, and K. Sacha, Phys. Rev. Lett. **120**, 140401 (2018).
[23] J. Zhang, P. W. Hess, A. Kyprianidis, P. Becker, A. Lee, J. Smith, G. Pagano, I. D. Potirniche, A. C. Potter, A. Vishwanath, N. Y. Yao, and C. Monroe, Nature **543**, 217 EP (2017).
[24] J. Rovny, R. L. Blum, and S. E. Barrett, Phys. Rev. Lett. **120**, 180603 (2018).
[25] S. Choi, J. Choi, R. Landig, G. Kucsko, H. Zhou, J. Isoya, F. Jelezko, S. Onoda, H. Sumiya, V. Khemani, C. von Keyserlingk, N. Y. Yao, E. Demler, and M. D. Lukin, Nature **543**, 221 EP (2017).
[26] K. Sacha and J. Zakrzewski, Reports on Progress in Physics **81**, 016401 (2017).
[27] H. J. Schulz, Phys. Rev. Lett. **65**, 2462 (1990).
[28] E. Arrigoni and G. C. Strinati, Phys. Rev. B **44**, 7455 (1991).
[29] A. P. Kampf, Phys. Rev. B **53**, 747 (1996).
[30] G. Salomon, J. Koepsell, J. Vijayan, T. A. Hilker, J. Nespolo, L. Pollet, I. Bloch, and C. Gross, Nature **565**, 56 (2019).
[31] P. J. D. Crowley, I. Martin, and A. Chandran, Phys. Rev. B **99**, 064306 (2019).
[32] I. Martin, G. Refael, and B. Halperin, Phys. Rev. X **7**, 041008 (2017).
[33] A. Verdeny, J. Puig, and F. Mintert, Zeitschrift für Naturforschung A **71**, 897 (2016).
[34] P. J. D. Crowley, I. Martin, and A. Chandran, Phys. Rev. B **99**, 064306 (2019).
[35] D. Cubero and F. Renzoni, Phys. Rev. E **97**, 062139 (2018).
[36] S. Nandy, A. Sen, and D. Sen, Phys. Rev. X **7**, 031034 (2017).
[37] S. Nandy, A. Sen, and D. Sen, Phys. Rev. B **98**, 245144 (2018).

- [38] S. Maity, U. Bhattacharya, A. Dutta, and D. Sen, Phys. Rev. B **99**, 020306 (2019).
- [39] R. Gommers, S. Denisov, and F. Renzoni, Phys. Rev. Lett. **96**, 240604 (2006).
- [40] D. Cubero and F. Renzoni, Phys. Rev. E **86**, 056201 (2012).
- [41] Y. Peng and G. Refael, Phys. Rev. B **98**, 220509 (2018).
- [42] A. Gangopadhyay, M. Dzero, and V. Galitski, Phys. Rev. B **82**, 024303 (2010).
- [43] S.-K. Son, S. Han, and S.-I. Chu, Phys. Rev. A **79**, 032301 (2009).
- [44] M. Senechal, *Quasicrystals and geometry* (CUP Archive, 1996).
- [45] (), additional requirement should be satisfied as well, e.g. the state at time t needs to be short-ranged correlated.
- [46] (), strictly speaking it is not the breaking of a symmetry but rather the long-range quasi-periodic order in time imprinted by the Hamiltonian drive. However, in analogy with the widely used TTSB we use the term QTTSB.
- [47] K. Giergiel, A. Kuroś, and K. Sacha, arXiv preprint arXiv:1807.02105 (2018).
- [48] F. M. Surace, A. Russomanno, M. Dalmonte, A. Silva, R. Fazio, and F. Iemini, Phys. Rev. B **99**, 104303 (2019).

Supplementary Material Rigidity of Discrete Time Quasi-Crystal Phase

The quasi-energy level statistics has been employed to determine the thermalisation phase transition point of DTCs [16, 20]. However, the perturbations we are concerned with here do not permit us to map it to a simple local PD Hamiltonian such that the Floquet operator and quasi-energies are not well-defined for the QPD system. Therefore, we study the perturbation's effects to DTQC in real time by ED up to 1000T, with trotter step $\Delta t = T/300$ with varying system size $L = 6, 8, 10, 12$, to analyse the thermalisation transition numerically.

Interaction perturbation

In order to check the stability of the DTQC given perturbative interactions, in Fig. 4, we check the amplitudes of the first subharmonic peak in the Fourier spectrum for various perturbations J_z as a function of different shifting time windows computed with 10 sites. FFT is done within 7 equally divided time windows between the domain $[300T, 1000T]$. Error bars are depicted according to the standard deviation of mean, σ/\sqrt{N} with N being the number of disorder realizations. Dotted lines are linear fits, of which the slopes γ capture the rate of decay of the signal due to thermalisation. The existence of a clear regime with $\gamma \sim 0$ (horizontal line) is crucial, confirming that the new phase is robust and does not heat up beyond the fine-tuned point of construction; while for larger J_z , amplitudes of the subharmonic behaviour drop and the system thermalises.

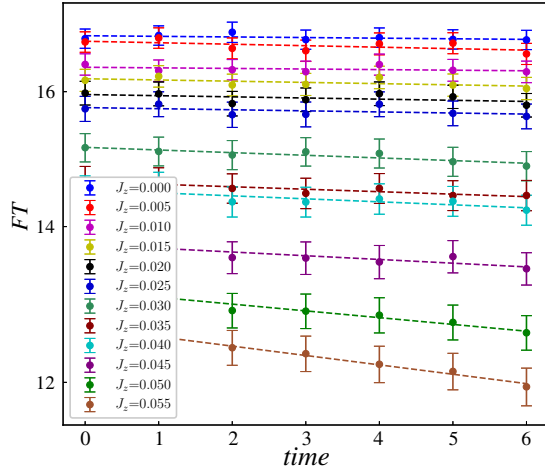


FIG. 4. Amplitudes of the first subharmonic peak of the Fourier spectrum of S_y for the DTQC on a log scale versus time (300 disorder configurations) for different interaction perturbations.

In order to investigate the relation between decay,

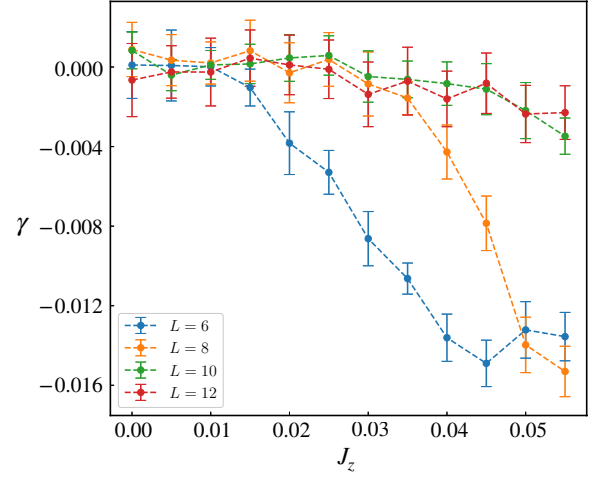


FIG. 5. Decay rate γ of the first subharmonic peak in Fourier spectrum versus perturbation J_z for varying system sizes. Decay γ remains zero for small perturbations and its drop indicates the transition to the thermalised phase. The transition point locates within $0.03 - 0.045$.

strength of perturbations, as well as finite size effects, we plot γ as a function of J_z for system sizes 6, 8, 10, 12 in Fig. 5. Each data point is obtained by averaging the γ calculated with varying lengths of FFT time window from 70 to 100T. The standard deviation is presented as error bar. After the stable regime with zero decaying rate, γ drops suggesting the onset of thermalisation. The critical value of the phase transition varies and becomes larger with the system size. A precise determination of the transition point is beyond the scope of this work.

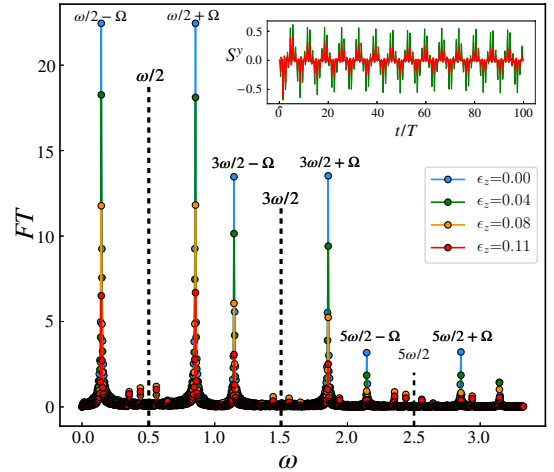


FIG. 6. Fourier transformation of the average magnetization in y direction of DTQC, computed by ED with 10 sites (300 disorder configurations) for different ϵ_z . FFT is done with 200-400 T. One gets new peaks at $k\omega/2 \pm \Omega$, indicating the existence of time quasi-crystal. Such a new phase will not be destroyed given perturbations as long as they are small. Inset is the dynamics for $\epsilon_z = 0.04, 0.11$.

Imperfect Rotation

Besides the perturbative interaction, we also consider the rotation perturbation and add $-h_2(t)\epsilon_z \sum_j \cos(\Omega t)\sigma_j^z$ to H_d in Eq. 12 with uniform strength ϵ_z . The Fourier spectrum is shown in Fig. 6 for various ϵ_z , and the inset shows the quasi-periodically oscillating evolution of $S^y(t)$. Similar as the previous case, subharmonic peaks are locked at $k\omega/2 \pm \Omega$ with descending heights for increasing perturbations. We find that for $\epsilon_z = 0.04$, the oscillations persist without decay up to at least $1000T$, while the rapid decay with $\epsilon_z = 0.11$ suggests that the system heats up quickly.

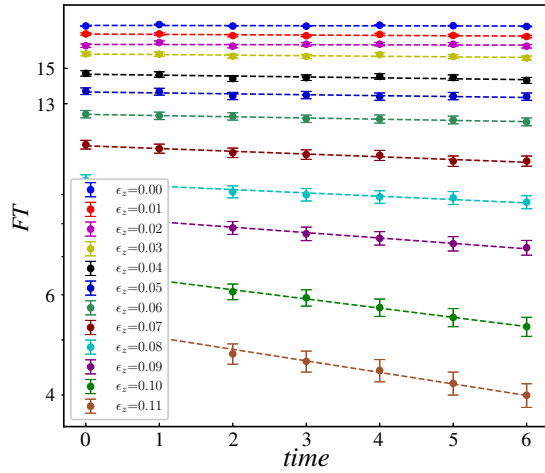


FIG. 7. Amplitudes of the first subharmonic peak of the Fourier spectrum of S_y for the DTQC on a log scale versus time (300 disorder configurations) for different pulse perturbations.

Long time behaviour of the first subharmonic peak computed with 10 sites for various perturbations are plotted in Fig. 7. The same method to obtain average and error bar is applied here as above, and a regime with zero γ can be observed. The relation between γ and ϵ_z is depicted in Fig. 8. The critical value of the thermal phase transition is approximately $\epsilon_z \sim 0.05$.

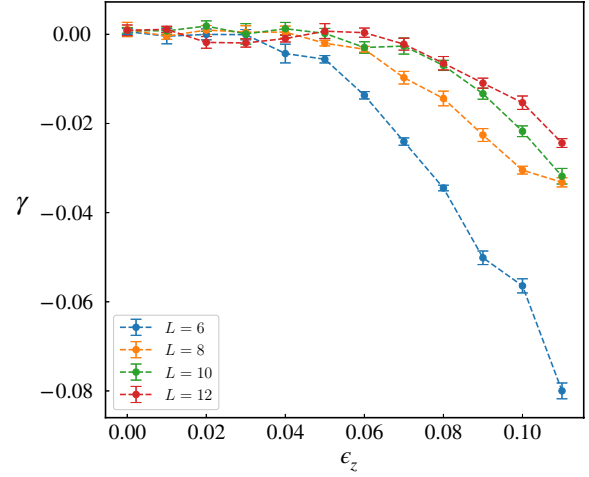


FIG. 8. Decay rate γ of the first subharmonic peak in Fourier spectrum versus perturbation ϵ_z for varying system sizes. γ remains zero for the DTQC and becomes negative for the thermalised phase, and the transition point locates around $\epsilon_z \sim 0.05$.